ChemPubSoc Europe

DOI: 10.1002/cphc.201600547

CHEMPHYSCHEM Articles

Investigation of the Effect of Thermal Annealing on Poly(3-hexylthiophene) Nanofibers by Scanning Probe Microscopy: From Single-Chain Conformation and Assembly Behavior to the Interfacial Interactions with Graphene Oxide

Sanrong Liu,[a] Xiaojing Ma,*[a] Bo Wang,[a] Xudong Shang,[a] Wenliang Wang,[a, b] and Xifei Yu*[a, b]

Poly(3-hexylthiophene) (P3HT) has been widely used in devices owing to its excellent properties and structural features. However, devices based on pure P3HT have not exhibited high performance. Strategies, such as thermal annealing and surface doping, have been used to improve the electrical properties of P3HT. In this work, different from previous studies, the effect of thermal annealing on P3HT nanofibers are examined, ranging from the single polymer chain conformation to chain packing, and the interfacial interactions with graphene oxide (GO) at nanoscale dimensions, by using scanning tunneling microscopy (STM), atomic force microscopy (AFM) and Kelvin probe force microscopy (KPFM). High-resolution STM images directly show the conformational changes of single polymer chains after thermal annealing. The morphology of P3HT nanofibers and the surface potential changes of the P3HT nanofibers and GO is further investigated by AFM and KPFM at the nanoscale, which demonstrate that the surface potentials of P3HT decrease, whereas that of GO increases after thermal annealing. All of the results demonstrate the stronger interfacial interactions between P3HT and GO occur after thermal treatments due to the changes in P3HT chain conformation and packing order.

1. Introduction

Poly(3-hexylthiophene) (P3HT) has attracted considerable attentions owing to its excellent electronic properties and good processability, and it has been widely used as the active layers in organic semiconductor devices, such as organic field-effect transistors (OFETs).[1–2] However, the charge carrier mobility of pure P3HT is usually low.[3] Thermal annealing is one of the strategies most used to improve the performance of P3HT-based OFETs.[4–10] It is known that ordered molecular packing of conductive polymer in films can lead to high charge transport and the 1D nanostructures of P3HT afford favorable carrier transport paths that improve device performance.[11–15] Thermal annealing can improve the molecular ordering and promote the formation of fibers in P3HT films, which results in higher electrical properties. However, this has been applied only to films formed by spin- or drop-coating, which is mostly used to prepare P3HT films. This is because films prepared in this way are actually a mixture of different P3HT assemblies caused by the uncontrolled solvent evaporation rate, flow and unconstrained P3HT chain movement[3] during spin- or drop-coating. Thermal annealing has been found to contribute to the formation of extended fibers and enhance the crystallinity of P3HT in these films.[5–10] However, for films that are formed of P3HT fibers, the influence of thermal annealing on the nanofibers, including the single-chain conformation, assembly behavior and their interactions with other materials, has not been studied.

Surface doping[16] is another method that can be used to improve the performance of P3HT-based OFETs, as it can improve the electrical contact in organic electronic devices due to the interfacial charge-transfer interactions between dopant and P3HT.[17] Graphene oxide (GO) is a newly reported p-type dopant for the surface of P3HT.[16] The use of GO has stimulated a lot of interest owing to its unique structures feature, electronic properties and solution processability.[16,18,19] Recent efforts have focused on P3HT and GO owing to the following reasons: 1) because the work function of GO falls within the band gap of P3HT,[20] there exist charge-transfer interactions between GO and P3HT; 2) GO possesses a two-dimensional (2D) plane structure with atom thickness, which facilitates charge generation and electron transfer;[19,21] and 3) GO is easily functionalized to make it soluble in organic solvents.[21] For example, Chen and co-workers firstly proposed that GO can be used as an acceptor material in a polymer-based organ-

[a] S. Liu, Dr. X. Ma, Dr. B. Wang, X. Shang, W. Wang, Dr. X. Yu
The Polymer Composites Engineering Laboratory
Changchun Institute of Applied Chemistry
Chinese Academy of Sciences
Changchun 130022 (China)
E-mail: xjma@ciac.ac.cn
xfyu@ciac.ac.cn

[b] W. Wang, Dr. X. Yu
University of Chinese Academy of Sciences Department
100049 Beijing (China)

ic photovoltaic (OPV) with P3HT as the electron donor, and found it worked well as the active layer in an OPV device; however, the best power conversion efficiency was only 1.4%.[1] Jen and co-workers demonstrated that the electrical conductivity of P3HT films can be increased by six orders of magnitude after a thin layer GO is deposited onto the films.[16] However, most of the recent studies have been focused on how to make use of the interactions between P3HT and GO.[19,22] Only little effort has been devoted to understanding and controlling the interactions between P3HT and GO. For example, Liscio and co-workers used Kelvin probe force microscopy (KPFM) to measure the surface potential (SP) of P3HT and reduced GO and reported that the there are no significant charge-injection barriers between them because of their small work function difference.[20] From our previous studies, we reported that GO can be doped differently if interacting with P3HT nanofibers of different nanostructures, as determined by combining spectroscopy with atomic force microscopy (AFM) and KPFM.[23] To understand and control the interfacial interactions between GO and P3HT at nanoscale dimensions is important not only because the interfacial doping can influence the electrical properties of P3HT but also it will enhance our knowledge in the area of interfacial engineering.

Thermal annealing has also been found to contribute to the enhancement of performance of devices based on GO-doped P3HT,[16,21] but detailed reasons have not been discussed or studied well. It is unknown why or how the thermal annealing can influence the P3HT nanofibers and their interfacial interactions with GO and these questions need to be further addressed.

Herein, and different to the previous studies, we used P3HT nanofibers as a model to study the effect of thermal annealing on single-chain conformation and assembly behavior. Then we focused on investigating and understanding the effect of thermal annealing on the interfacial interactions between P3HT and GO, and the reasons for them at the nanoscale. We extract nanoscale information by providing single polymer chain conformation, nanomorphology and nanosurface potential, and give valuable information on how to effectively control the interactions of P3HT nanofibers with GO by changing external conditions.

Experimental Section

Materials

Regioregular P3HT ($M_n = 29.9\ kg\ mol^{-1}$, polydispersity index = 1.27) was purchased from Rieke Metals Inc. (Lincoln, USA) and used without further purification. Head-to-tail regioregularity was determined using nuclear magnetic resonance to be about 98% by comparing the signals at 2.8 and 2.6 ppm.[24] GO was prepared according to a modified Hummers' method.[25] Graphite powders were purchased from Sinopharm Chemical Reagent Co. Ltd. (Changchun, China). Chloroform and THF were purchased from Beijing Chemical Reagents Company (Beijing, China).

Preparation of P3HT Nanofibers on GO-Coated Substrates

P3HT ($1.2\ mg\ mL^{-1}$) was dissolved in chloroform, and stirred at 70 °C. After the P3HT was completely dissolved and the solution became clear and orange, the P3HT solution was cooled to room temperature. Then, THF, a relatively poor solvent was added into prepared solution. The solution was placed in the dark for one day to reach final equilibrium.

Silicon wafers and quartz plates were cleaned in boiling piranha solution (H_2SO_4/H_2O_2 7:3), rinsed with ultrapure water and dried under a ultrahigh-purity nitrogen stream.

A drop of GO solution were firstly dropped onto the substrates and left on for 30–60 min. Then the substrates were dipped into the P3HT nanofiber solutions for different times followed by dropping into the corresponding solvent. All the samples were used within several days after preparation.

Thermal Annealing

For the thermal annealing, the sample prepared as above was baked at 160 °C for 20 min on a hot plate under a nitrogen atmosphere.

Characterization

UV/Vis absorption spectra were recorded on a Shimadzu UV-3600 spectrophotometer. Differential scanning calorimetry (DSC) was measured at a heating rate of $20\ °C\ min^{-1}$ under nitrogen atmosphere on a TA Instruments Q200 calorimeter.

KPFM, AFM and scanning tunneling microscopy (STM) were performed using Multimode Nanoscope IIIA instrument (Bruker). KPFM was performed in the lift mode and the images were recorded using a conductive SCM-PIT probe (Bruker, Pt/Ir-coated Si with frequency ≈ 75 kHz and nominal tip radius ≤ 20 nm). AFM imaging was performed using a silicon cantilever with the resonant frequency of 300–400 kHz and radius of < 10 nm. STM measurements were performed on a freshly cleaved HOPG (quality ZYB) surface. Mechanically formed Pt/Ir (80:20) tips were used and all the images were recorded in the constant-current mode, and the specific tunneling conditions are given in the figure captions.

2. Results and Discussion

Figure 1 shows the UV/Vis spectra of the P3HT–GO composites before and after thermal treatment. It has been reported that the degree of intrachain order can be manifested in the absorption spectrum of P3HT.[26–28] The absorbance ratio of the lowest energy peak to the next replica peak, A_{0-0}/A_{0-1}, will increase if the degree of intrachain order increases.[14] The A_{0-0}/A_{0-1} peak ratio obtained from UV/Vis spectra increased from 0.724 to 0.772 after heating treatment, which suggested the improved crystallinity in the side chain and in the π–π stacking direction.[26–28] Also, the peak at about 600 nm can be assigned to the P3HT crystalline domain,[1] and the change of molecular interactions can lead to shifts in the absorption spectrum and a change in the peak intensities.[14] As shown in Figure 1, a more intense absorbance peak at 600 nm was displayed after

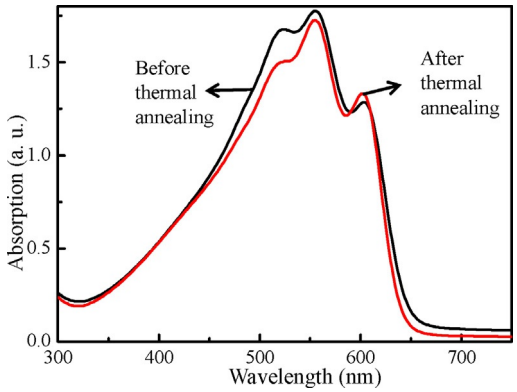

Figure 1. UV/Vis absorption spectra of P3HT before and after thermal annealing.

thermal annealing, which might suggest that P3HT nanofibers interact with GO with a stronger intensity owing to its enhanced crystallinity in the side chain and intrachain order[23] induced by thermal treatment.

To further verify that thermal treatment improved crystallinity in the side chains and led to more ordered packing in the main backbones, differential scanning calorimetry (DSC) was conducted to measure the melting temperature and the heat of fusion of P3HT nanofibers (Figure 2). The exothermic peaks

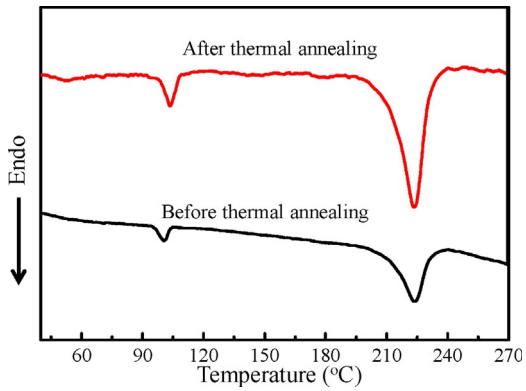

Figure 2. DSC thermograms of P3HT nanofibers before and after thermal annealing.

at about 224 and 104 °C correspond to the melting temperatures of the P3HT main backbones and side chains, respectively.[29] The data shows that the melting temperature of the P3HT main chains was essentially the same before and after thermal annealing, but the heat of fusion increased from 7.1 to 12.2 $W g^{-1}$, whereas the melting temperature of the annealed side chains increased from 102 to 105 °C, and the corresponding heat of fusion increased from 0.9 to 2.4 $W g^{-1}$. Because the annealing temperature used in our temperature is 160 °C, which is above the melting temperature of the P3HT alkyl side chains, it can lead to the re-assembly of the side chains in a P3HT polymer chain and result in improved intrachain order and interchain interactions in alkyl side chain directions. Although 160 °C is lower than the melting temperature of the main backbones in P3HT nanofibers, the increase in the heat of fusion indicated that the interactions between main backbones are also improved. These results demonstrate that the packing order of both the main backbones and side chains in P3HT nanofibers were improved after thermal treatment, which is consistent with the increased A_{0-0}/A_{0-1} peak ratio obtained from UV/Vis spectroscopic measurements and the results reported in the literature.[29]

In order to better understand the change of P3HT after thermal treatment, the single P3HT chain conformation and packing order on the nanometer scale were further investigated by STM and AFM. STM is a powerful technique for studying molecule conformation and molecular interactions because of its high structural resolution. It has been used to probe the self-assembled structure and chain folding of polymers with sub-molecular-level resolution.[30] In this work, we used STM to investigate the change of chain conformation and assembly behavior of the polymer chain before and after thermal annealing. Three prominent features are shown in STM images (Figure 3) acquired after thermal treatment: the first is the en-

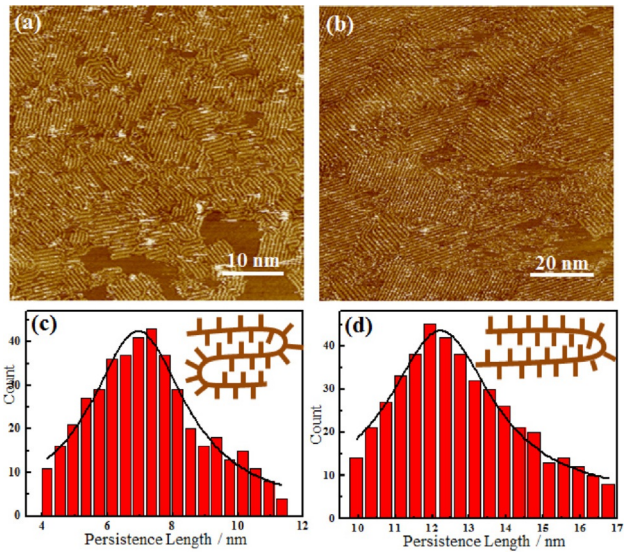

Figure 3. STM images of P3HT adsorbed at HOPG at a) room temperature and b) 160 °C. Statistic histograms of the persistence length of P3HT c) before and d) after thermal annealing; inset: schematic model representations of P3HT chain conformations before and after annealing treatments. The imaging conditions were $I = 518.2$ pA and $V = -819$ mV.

larged area of the domains in which the polymer chains are aligned in the same direction. It is known that polymer chains generally follow a three-fold symmetry orientation promoted by the epitaxial effects on highly oriented pyrolytic graphite (HOPG).[30] However, polymer chains with the same orientations might not be in the same domains shown in Figure 3a. To increase the areas of domains in which P3HT chains are distributed in the same domain, more energy is needed, as this is an entropy-reducing process. Heating provides the P3HT chains enough energy to overcome the previous interactions between P3HT and HOPG to move into the same orientation as

the neighboring polymer chains, which facilitates the stronger interchain interactions, except for the interactions between P3HT and HOPG. The second feature is that the persistence length of a single P3HT chain is increased from 7.5 to 12.0 nm after thermal treatment as shown in the static histograms in Figure 3c and 3d. The third feature is that the ratio of the amount of P3HT chains with linear structures to that of folded chains (N_L/N_f) increased from 0.76 (43.2%/56.8%) to 7.13 (87.7%/12.3%). Schematic models (Figure 3c and 3d, inset) were drawn to directly show the conformation change of a single P3HT chain before and after thermal treatment. Therefore, it can be proposed that thermal treatments enhance the planar conformation of segments that favor the formation of extended structures in which the π electrons are more delocalized, which were quantified by the change in persistence length and the ratio of linear and folded chains. Taking together the increased persistence length and N_L/N_f ratio with the increased heat fusion of the main backbones and side chains revealed by DSC experiments, it can be concluded that thermal treatment changed the P3HT chain conformation and consequently the intrachain interactions, which is consistent with the UV/Vis spectroscopy results.

In addition, to further observe how the single P3HT chain changed with temperature, STM measurements at 200 °C were also performed (Figure 4). This temperature is slightly lower than the melting temperature of the P3HT main chains in bulk

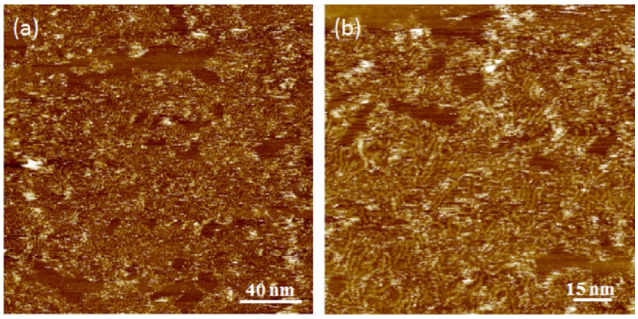

Figure 4. Large-scale and high-resolution STM images of P3HT adsorbed on HOPG at 200 °C.

film. Because the sample for STM measurements is thin and usually a monolayer, we believe that this temperature might be, or close to, the melting temperature of the P3HT monolayer. Samples were prepared as follows: after the samples were heated to 200 °C, they were put into the liquid nitrogen immediately to retain as much as possible the original conformations at 200 °C. Then, STM measurements were immediately performed to detect the conformation of P3HT. It should be noted that the conformation will deviate from the original conformations at 200 °C if the samples for STM measurements are kept at room temperature for some time, and the more they will change the longer they are kept at room temperature. The image shown in Figure 4 is obtained immediately after they were just taken out of the liquid nitrogen. It can be seen from Figure 4 that P3HT chains at 200 °C were nearly disordered and it is impossible to obtain high-resolution images because 200 °C is nearly the melting temperature of the main backbones and at that temperature the P3HT chains began moving on the substrates.

The effects of different annealing temperatures on P3HT films were also observed, and morphology changes were recorded by AFM. It can be seen from Figure 5 that at room tem-

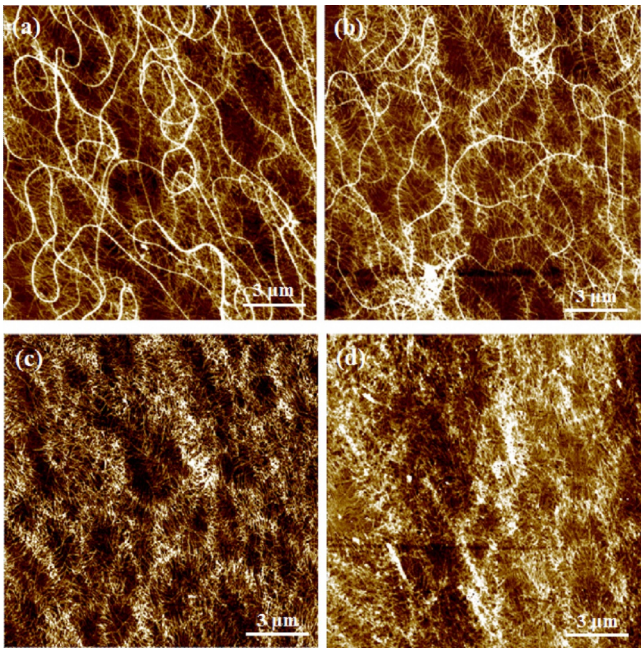

Figure 5. AFM images of P3TH films at different temperatures: a) room temperature, b) 100, c) 140, and d) 220 °C.

perature the P3HT self-assembled into many fibers with different diameters (Figure 5a). After the films were heated to 100 °C, the morphology of P3HT films was mostly retained (Figure 5b). If the films were heated to 140 °C, the fibers with larger diameters nearly disappeared, whereas the small fibers were retained (Figure 5c). If the films were heated to 220 °C, the resolutions of the images are lower than those of the P3HT films at other temperatures (Figure 5d). This might be caused by the movement of P3HT chains at different temperatures. It is known that single P3HT molecules assemble into fibers owing to the π–π interactions between the main backbone and that these P3HT fibers further assemble into larger fibers because of the interactions between the alkyl chains.[11,12,31] In our experiments, if the samples were heated to 160 °C, the alkyl chains began to move, which decreased the interactions between small fibers and finally the large fibers disassemble. As the films are further heated to 220 °C, the main backbones of the P3HT begin to move, which renders the small fibers unstable. This might be the reason why the clarity of the AFM images of the P3HT film at 220 °C is lower than those of films at other temperatures.

To further investigate the effect of thermal treatment on the interfacial interactions of P3HT nanofibers and GO, SPs were measured by KPFM. KPFM can be used to simultaneously

sample topography and electric potential on the nanometer scale. In KPFM experiments, the conductive AFM probe is used as an electrode to determine the surface contact potential difference between the AFM probe and the sample at nanometer dimensions.[32,36] It has been used to investigate the electronic properties of films[33–35] and their charge-transport interactions.[20,23] Figure 6 displays the AFM and corresponding KPFM

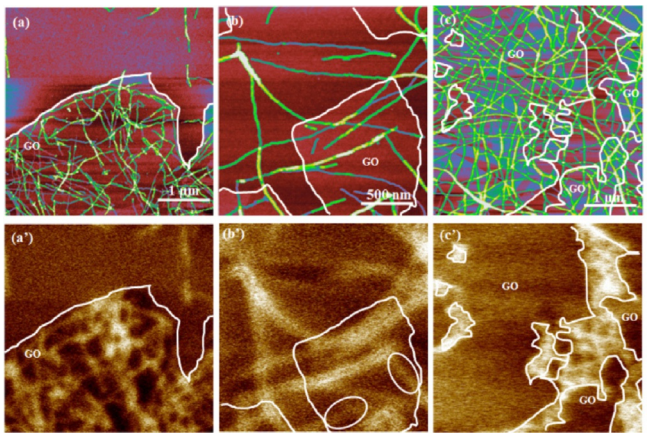

Figure 6. KPFM (top) and AFM (bottom) images of P3HT-GO nanocomposites before (a and a′) and after (b and b′, c and c′) thermal annealing. P3HT nanofibers imaged in a, a′, b, and b′ were adsorbed on the top of GO surface, whereas in c and c′ GO was dropped onto the P3HT surface. The white ellipses in b′ indicate fibers with different SP contrasts.

images of P3HT nanofibers on GO before and after heating. To accurately determine the SP changes of P3HT and GO before and after thermal treatments, two kinds of films were prepared: in one, the P3HT nanofibers were adsorbed onto the GO surface (Figure 6b and 6b′) and the other was vice versa (Figure 6c and 6c′), which make it possible to measure the SP of both the P3HT and GO after thermal treatment with more precision. For simplicity, the substrate (SiO_2) was used as a reference, and its SP value was set to zero. Figure 7 shows in detail the SP values of the P3HT and GO before and after annealing. P3HT nanofibers showed a brighter contrast in all the KPFM images (Figure 6). Before thermal annealing (Figure 6a′), GO showed a darker contrast compared with that of the SiO_2 substrates, which was found to be between approximately 16 and 29 mV. It should be mentioned that the SP of P3HT nanofibers decreased after interaction with GO (white elliptical outlines in Figure 6b″), which is consistent with our previous results.[23] The most interesting things are that if GO was deposited onto the surface of the P3HT nanofibers, the SPs values of GO were found to be greatly improved (Figure 5c″). The SP of P3HT also increased after thermal treatment. However, the increase for P3HT was smaller than that of GO, which means the SP difference between P3HT and GO after thermal treatments was decreased and the SP values of P3HT and GO after thermal treatments were closer to each other compared with those before annealing.

It has been found that the SP values measured in very thin films are actually the coordinated result of the interactions be-

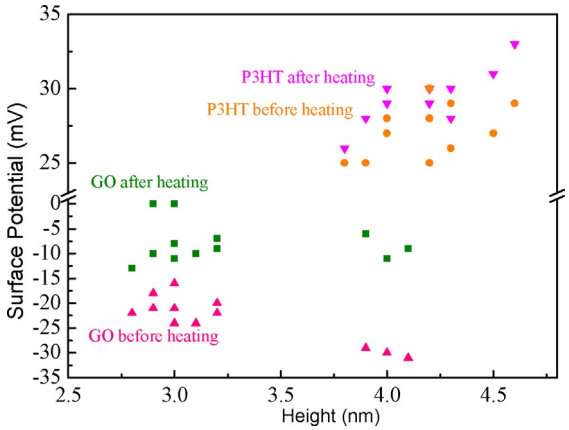

Figure 7. Statistical analysis of the SPs of P3HT and GO before and after annealing.

tween the layers and substrates below.[20] Therefore, in our case the measured SP values of P3HT should be the result of P3HT interacting with GO instead of the absolute SP values of P3HT, and the same logic can also be applied to GO. It is known that subtle changes in the structure can lead to the redistribution of charge, consequently changing the electronic properties of the materials.[36] The UV/Vis spectroscopy and AFM data directly showed that the intrachain order and crystallinity of P3HT was improved after thermal annealing, which suggests that the SP of P3HT changed after thermal annealing. Gao et al. found that the conductivity of P3HT can be increased by six orders of magnitude after a thin layer of GO sheets were deposited on the P3HT film, and they attributed this increase in conductivity to the proton doping of the surface of P3HT by GO.[16] The protons come from the functional groups in GO, including carboxyl, hydroxy and phenol groups. It is known that heating can promote release of such protons and results in higher proton density, which can lead to stronger doping interactions between P3HT and GO. We also found that heating P3HT without GO and heating GO without P3HT has no such effect on their SP values. All these results demonstrated that dipoles at the interface between P3HT and GO were enhanced by the thermal treatment.

3. Conclusions

A combination of UV/Vis spectroscopy, DSC, STM, AFM and KPFM studies showed that the intrachain order in single P3HT fibers was improved after thermal treatment and that the single P3HT chain is prone to absorb onto GO in a less-folded or even linear conformation, which results in improved delocalization of electrons along the main backbone, stronger π–π interactions between P3HT chains and formation of P3HT fibers with more order. In addition, KPFM results further showed that the SPs of P3HT nanofibers and GO are greatly changed by the interaction with each other and the SP difference of P3HT nanofiber and GO is reduced after heating, which demonstrated that stronger interfacial doping between them occurred. Finally, we investigated the thermal effect on the single polymer

chain conformation, intrachain order and crystallinity of P3HT nanofibers and the corresponding stronger interfacial interactions between P3HT and GO at nanoscale dimensions. The strengthening of the interfacial interactions should originate from the synergistic effects of more ordered chain packing in P3HT fibers and altered SP of P3HT and GO after thermal treatment. These findings can provide in-depth analysis and understanding of the effects of thermal annealing on P3HT-based devices, contribute to knowledge on the topic of conductive polymer materials, and provide more information on how to prepare devices with higher performance.

Acknowledgements

Financial support from the National Natural Science Foundation of China (21304096, 21474103) is acknowledged.

Keywords: atomic force microscopy · graphene oxide · poly(3-hexylthiophene) · scanning tunneling microscopy · thermal annealing

[1] W. D. Oosterbaan, J.-C. Bolsee, A. Gadisa, V. Vrindts, S. Bertho, J. D'Haen, T. J. Cleij, L. Lutsen, C. R. McNeill, L. Thomsen, J. V. Manca, D. Vanderzande, *Adv. Funct. Mater.* **2010**, *20*, 792 – 802.
[2] J.-Y. Chen, C.-C. Kuo, C.-S. Lai, W.-C. Chen, H.-L. Chen, *Macromolecules* **2011**, *44*, 2883 – 2892.
[3] S.-Y. Min, Y.-H. Kim, C. Wolf, T.-W. Lee, *ACS Appl. Mater. Interfaces* **2015**, *7*, 18909 – 18914.
[4] S. Cho, K. Lee, J. Yuen, G. Wang, D. Moses, A. J. Heeger, M. Surin, R. Lazzaroni, *J. App. Phy.* **2006**, *100*, 114503.
[5] I. Roy, S. Hazra, *RSC Adv.* **2015**, *5*, 665 – 675.
[6] S.-J. Kang, S. Song, C. Liu, D.-Y. Kim, Y.-Y. Noh, *Org. Electron.* **2014**, *15*, 1972 – 1982.
[7] Z. Gu, T. Kanto, K. Tsuchiya, T. Shimomura, K. Ogino, *J. Polym. Sci. Part A* **2011**, *49*, 2645 – 2652.
[8] Y. Kim, S. A. Choulis, J. Nelson, D. D. C. Bradley, S. Cook, J. R. Durrant, *Appl. Phys. Lett.* **2005**, *86*, 063502.
[9] D. H. Kim, Y. D. Park, Y. Jang, H. Yang, Y. H. Kim, J. I. Han, D. G. Moon, S. Park, T. Chang, C. Chang, M. Joo, C. Y. Ryu, K. Cho, *Adv. Funct. Mater.* **2005**, *15*, 77 – 82.
[10] R. C. Hiorns, R. de Bettignies, J. Leroy, S. Bailly, M. Firon, C. Sentein, A. Khoukh, H. Preud'homme, C. Dagron-Lartigau, *Adv. Funct. Mater.* **2006**, *16*, 2263 – 2273.
[11] S. Samitsu, T. Shimomura, S. Heike, T. Hashizume, K. Ito, *Macromolecules* **2008**, *41*, 8000 – 8010.
[12] J. Liu, M. Arif, J. Zou, S. I. Khondaker, L. Zhai, *Macromolecules* **2009**, *42*, 9390 – 9393.
[13] M. Brinkmann, *J. Polym. Sci. Part B* **2011**, *49*, 1218 – 1233.
[14] J. D. Roehling, I. Arslan, A. J. Moule, *J. Mater. Chem.* **2012**, *22*, 2498 – 2506.
[15] A. Liscio, V. Palermo, P. Samori, *Adv. Funct. Mater.* **2008**, *18*, 907 – 914.
[16] Y. Gao, H.-L. Yip, K.-S. Chen, K. M. O'Malley, O. Acton, Y. Sun, G. Ting, H. Chen, A. K.-Y. Jen, *Adv. Mater.* **2011**, *23*, 1903 – 1908.
[17] W. Chen, D. Qi, X. Gao, A. T. S. Wee, *Prog. Surf. Sci.* **2009**, *84*, 279 – 321.
[18] M. M. Stylianakis, E. Stratakis, E. Koudoumas, E. Kymakis, S. H. Anastasiadis, *ACS Appl. Mater. Interfaces* **2012**, *4*, 4864 – 4870.
[19] Q. Liu, Z. Liu, X. Zhong, L. Yang, N. Zhang, G. Pan, S. Yin, Y. Chen, J. Wei, *Adv. Funct. Mater.* **2009**, *19*, 894 – 904.
[20] A. Liscio, G. P. Veronese, E. Treossi, F. Suriano, F. Rossella, V. Bellani, R. Rizzoli, P. Samori, V. Palermo, *J. Mater. Chem.* **2011**, *21*, 2924 – 2931.
[21] Z. Liu, Q. Liu, Y. Huang, Y. Ma, S. Yin, X. Zhang, W. Sun, Y. Chen, *Adv. Mater.* **2008**, *20*, 3924 – 3930.
[22] G. Eda, M. Chhowalla, *Nano Lett.* **2009**, *9*, 814 – 818.
[23] S. Liu, X. Ma, B. Wang, X. Shang, W. Wang, X. Yu, *Macromolecules* **2015**, *48*, 5791 – 5798.
[24] H. Sirringhaus, P. J. Brown, R. H. Friend, M. M. Nielsen, K. Bechgaard, B. M. W. Langeveld-Voss, A. J. H. Spiering, R. A. J. Janssen, E. W. Meijer, P. Herwig, D. M. de Leeuw, *Nature* **1999**, *401*, 685 – 688.
[25] W. S. Hummers, R. E. Offeman, *J. Am. Chem. Soc.* **1958**, *80*, 1339 – 1339.
[26] F. C. Spano, *Chem. Phys.* **2006**, *325*, 22 – 35.
[27] F. C. Spano, *J. Chem. Phys.* **2005**, *122*, 234701.
[28] J. F. Chang, J. Clark, N. Zhao, H. Sirringhaus, D. W. Breiby, J. W. Andreasen, M. M. Nielsen, M. Giles, M. Heeney, I. McCulloch, *Phys. Rev. B* **2006**, *74*, 115318.
[29] C.-M. Fu, K.-S. Jeng, Y.-H. Li, Y.-C. Hsu, M.-H. Chi, W.-B. Jian, J.-T. Chen, *Macromol. Chem. Phys.* **2015**, *216*, 59 – 68.
[30] E. Mena-Osteritz, A. Meyer, B. M. W. Langeveld-Voss, R. A. J. Janssen, E. W. Meijer, P. Bauerle, *Angew. Chem. Int. Ed.* **2000**, *39*, 2679 – 2684; *Angew. Chem.* **2000**, *112*, 2791 – 2796.
[31] J. Liu, I. A. Mikhaylov, J. Zou, I. Osaka, A. E. Masunov, R. D. McCullough, L. Zhai, *Polymer* **2011**, *52*, 2302 – 2309.
[32] A. Liscio, V. Palermo, P. Samori, *Acc. Chem. Res.* **2010**, *43*, 541 – 550.
[33] J. Lü, L. Eng, R. Bennewitz, E. Meyer, H. J. Güntherodt, E. Delamarche, L. Scandella, *Surf. Interface Anal.* **1999**, *27*, 368 – 373.
[34] V. Palermo, M. Palma, Z. Tomovic, M. D. Watson, R. Friedlein, K. Mullen, P. Samori, *ChemPhysChem* **2005**, *6*, 2371 – 2375.
[35] V. Palermo, A. Liscio, M. Palma, M. Surin, R. Lazzaroni, P. Samori, *Chem. Commun.* **2007**, 3326 – 3337.
[36] M. Baghgar, A. M. Barnes, E. Pentzer, A. J. Wise, B. A. G. Hammer, T. Emrick, A. D. Dinsmore, M. D. Barnes, *ACS Nano* **2014**, *8*, 8344 – 8349.

Manuscript received: May 24, 2016
Accepted Article published: July 28, 2016
Final Article published: August 18, 2016